**PHYSICS AND CHEMISTRY OF SOLID STATE**
V. 25, No. 4 (2024) pp. 757-763

*Section: Technology*

**DOI: 10.15330/pcss.25.4.757-763**

*Vasyl Stefanyk Precarpathian National University*

**ФІЗИКА І ХІМІЯ ТВЕРДОГО ТІЛА**
**Т. 25, № 4 (2024) С. 757-763**

*Технічні науки*

PACS: 42.79.Pw; 07.57.Kp

ISSN 1729-4428 (Print)
ISSN 2309-8589 (Online)

Ruslan Politanskyi[1], Igor Kogut[2], Maria Vistak[3], Zinoviy Mykytyuk[4], Olha Shymchyshyn[4], Ivan Diskovskyi[3]

# Modelling of a multilayer high-tech film for an infrared photodetector (3.5-5.0 µm)

[1]*Yuriy Fedkovych Chernivtsi National University, Chernivtsi, Ukraine*
[2]*Vasyl Stefanyk Precarpathian National University, Ivano-Frankivsk, Ukraine, igor.kohut@pnu.edu.ua*
[3]*Danylo Halytsky Lviv National Medical University, Lviv, Ukraine*
[4]*Lviv Polytechnic National University, Lviv, Ukraine*

The paper investigates the properties of an antireflective film for a photodetector made of indium antimonide (InSb), configured for transmission in the infrared range (3.5-5.0 µm), which coincides with the absorption peak of carbon dioxide ($CO_2$). The film is a four-layer coating formed by the following materials: silicon dioxide ($SiO_2$), silicon monoxide (SiO), silicon suboxide ($SiO_{1<x<2}$) and silicon (Si), which are placed in the order of increasing refractive index: 1.45, 1.9, 2.6 and 3.2. In this way, the film provides an increase in the refractive index from 1 to a value close to the refractive index of the active material of the photodiode (4.0). The matrix method is used to calculate the complex light reflection coefficient for perpendicular and parallel polarization in the range of wavelengths and angles of incidence on the film surface that correspond to the characteristics of the infrared radiation sensor. The range of angles is selected based on the geometric characteristics of the infrared non-dispersive sensor AK9710ADF01 developed by Asahi Kasei. The spectral composition of the light is determined by the characteristics of the L15895 series infrared LED manufactured by the Hamamatsu company. As a result of the conducted research, the optimal values of the thicknesses of the layers are calculated, which provide a reflection coefficient of 22% for unpolarized radiation, which is compared to the values that are characteristic of modern infrared photodetectors. At the same time, it is concluded that the values of the reflection coefficient are significantly higher for waves with parallel polarization (by 40% at the central wavelength) than for waves with perpendicular polarization.

**Keywords:** Wave interference, matrix method, infrared sensor, infrared LED.

*Received 18 August 2024; Accepted 24 November 2024.*

## Introduction

Optical film materials are necessary and one of the most important components of the production of solar energy materials and infrared detectors. The production technology of anti-reflective coatings involves two fundamentally different ways of their construction: multilayer thin films [1] or one layer made of porous silicon with different degrees of porosity and pore orientation [2]. The interference principle of reducing the power of reflected radiation applies to the indicated methods of manufacturing anti-reflective films. Modern commercial photodetectors use almost just such films. They are made mainly from classic semiconductor materials that have been used for a long time: Si, Ge, HgCdTe and InGaAs. Such sensors require external power supply, which limits the possibility of their application in the Internet of Things (IoT) technologies [3]. Technologies for manufacturing nanostructured surfaces and surfaces with plasmons are complex and can lead to the destruction of the photodiode structure [3]. Therefore, classic multilayer films with close values of lattice coefficients and a smooth change in refractive index remain in the field of view of manufacturers of optical range detectors.

Therefore, active searches are being conducted for

materials and design solutions for optical range sensors that do not require external power sources. The basis of such sensors are two-dimensional materials that have a better quantum yield than bulk materials and significantly less or no external energy consumption. The most common materials for the production of two-dimensional films are: graphene, dichalcogenides of transition metals (molybdenum disulphide $MoS_2$), MXenes (materials consist of a layer of atomic carbon located between two layers of a transition metal), metal oxides that can form a two-dimensional film: $SnO_2$, $Ga_2O_3$, $In_2O_3$, PbO and $Bi_2O_3$, oxides of transition metals: $MoO_2$, $HfO_2$, $WO_3$, $V_2O_5$ and $Cr_2O_3$ and semi-metallic oxides: $GeO_2$ and $TeO_2$ [4, 5, 6]. Other technologies of anti-reflective mechanisms that use the polarization properties of light [7] and nanostructured anti-reflective surfaces [8] have also been developed. These technologies emerged relatively recently, they are much more complex and require further improvement.

# I. Structure Materials and methods

### 1.1. Materials of anti-reflective films and protective coating for photodiode production

Indium antimonide InSb is one of the most effective materials for manufacturing photodetectors of infrared radiation. The refractive index of this material in a wide range of wavelengths (from visible to infrared) is 4. This causes a high reflection coefficient, and therefore anti-reflection coatings must be used in the design of the photodetector. Effective for the application of a photodetector based on indium antimonide is a 4-layer coating, which is described in detail in [9]. Its structure is formed by materials that are well-matched to each other in terms of their lattice parameters and manufacturing technology, and the refractive indices are such that there is a jump-like increase in this index from the refractive index of the external environment to the refractive index of InSb. The scheme of the layer is shown in Fig. 1.

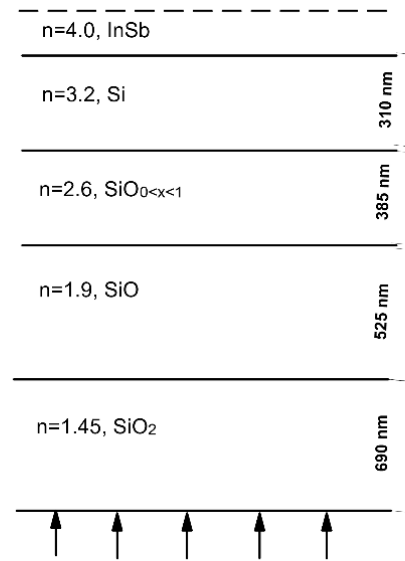


**Fig. 1.** Scheme of antireflective coating for indium antimonide (InSb) [9].

It consists of silicon dioxide ($SiO_2$) with a refractive index n=1.45; silicon monoxide (SiO) with a refractive index n=1.9; silicon suboxide ($SiO_{0<x<1}$) with a refractive index n=2.6 and silicon (Si) with a refractive index n=3.2. The thickness of each layer is selected from the condition of the maximum illuminating capacity of each layer, that is, the equality of the optical thickness of the layer of the fourth wavelength of the incident wave, which is chosen according to the spectral power density of the infrared radiation source:

$$\begin{cases} d_1 = \frac{\lambda_0}{4 \cdot n_1} = \frac{4300}{4 \cdot 1.45} \approx 740\ nm;\ d_2 = \frac{\lambda_0}{4 \cdot n_2} = \frac{4300}{4 \cdot 1.90} \approx 565\ nm \\ d_3 = \frac{\lambda_0}{4 \cdot n_3} = \frac{4300}{4 \cdot 2.60} \approx 415\ nm;\ d_4 = \frac{\lambda_0}{4 \cdot n_4} = \frac{4300}{4 \cdot 3.20} \approx 335\ nm \end{cases} \quad (1)$$

In work [9], a thin passivating layer of silicon nitride is added between the anti-reflective layer and the light-receiving surface of the photodiode, which is necessary for using the device in a wide range from infrared to visible light. We are considering a device tuned to a narrow band of the optical range with a central frequency of 4.3 μm, so we do not use a passivating layer.

### 1.2. Matrix method of calculating transmission coefficients

The matrix method is based on determining the phases of waves that propagate in a multilayer anti-reflective coating.

The parameters of this method are the wavelength and the angle of incidence on the first layer of the film. This method uses different formulas for waves with one of two types of polarization: in the plane of incidence (vertical polarization) and in the plane perpendicular to it (horizontal polarization). The method is based on the application of the interference matrices of each individual layer $M^j$ of dimension $2 \times 2$. The process of wave passage is described by the matrix product of each layer, starting from the outer one:

$$\begin{cases} M^j = \begin{pmatrix} m_{11}^j & m_{12}^j \\ m_{21}^j & m_{22}^j \end{pmatrix} \\ M = \prod_{i=1}^{n} M^{(n-i)} = M^n \times M^{n-1} \times \ldots \times M^1 \end{cases} \quad (2)$$

The matrix method determines the interference interaction of rays propagating in a multilayer structure. The phase thickness of each layer determines the length of the wave's optical path and its phase change. The matrix coefficients contain the phase thickness content of each layer, which is determined by its thickness $d_j$ and the optical permeability of the layer $n_j$, the wavelength λ, the angle $\alpha_j$ of wave propagation in the layer, the value of

which also depends on the type of wave polarization: perpendicular (symbol "s") or parallel ( symbol "p") polarization:

$$\varphi_j = 2\pi \times \frac{n_j d_j cos(\alpha_j)}{\lambda} \quad (3)$$

The matrix method is based on determining the phases of waves that propagate in a multilayer anti-reflective coating.

The matrix coefficients for both types of polarization are determined by the phase thickness of the layer $\varphi_j$, its optical permeability $n_j$, and the angle at which the beam propagates in this layer $\alpha_j$. They also depend on the type of wave polarization:

$$\begin{cases} m^j_{11(s,p)} = cos(\varphi_j) \\ m^j_{12(s)} = i \cdot sin(\varphi_j)/n_{j(s,p)} \\ m^j_{21(s,p)} = i \cdot sin(\varphi_j) \times n_{j(s,p)} \\ m^j_{22(s,p)} = cos(\varphi_j) \end{cases}, \quad (4)$$

where $i$ is an imaginary unit;

$$\begin{cases} n_{j(s)} = cos(\alpha_j) \\ n_{j(p)} = \frac{n_j}{cos(\alpha_j)} \end{cases}. \quad (5)$$

We determine the propagation angles of electromagnetic waves in each layer using Snellius' law:

$$\begin{cases} sin(\alpha_0)/n_0 = sin(\alpha_1)/n_1 \\ \dots \\ sin(\alpha_{n-1})/n_{n-1} = sin(\alpha_n)/n_n, \\ sin(\alpha_n)/n_n = sin(\alpha_s)/n_s \end{cases} \quad (6)$$

where $\alpha_0$ is the angle at which the wave falls on the surface of the device, $n_0$ is the refractive index of the external medium, $\alpha_s$ is the angle at which the wave leaves the last layer of the anti-reflective coating, $n_s$ is the refractive index of the active medium of the device.

As a result of matrix multiplication (2), one resulting matrix is formed with two real and two imaginary coefficients:

$$M_{(s,p)} = \begin{pmatrix} m_{11(s,p)} & i \cdot m_{12(s,p)} \\ i \cdot m_{21(s,p)} & m_{22(s,p)} \end{pmatrix}.$$

Knowing these coefficients, we determine the complex reflection coefficient for waves with both parallel and perpendicular polarizations:

$$r_{(s,p)} = \frac{(n_0 m_{11(s,p)} - n_s m_{22(s,p)}) + i \cdot (n_0 n_s m_{12(s,p)} - m_{21(s,p)})}{(n_0 m_{11(s,p)} + n_s m_{22(s,p)}) + i \cdot (n_0 n_s m_{12(s,p)} + m_{21(s,p)})} \quad (7)$$

The total reflection coefficient $R$ depends on the degree of polarization of the incident radiation, and is a function of two variables: the angle of incidence on the surface of the device and the wavelength of the incident radiation. If the light source generates unpolarized radiation, then its value is determined as the average value of the coefficients $|r_{(s)}|^2$ and $|r_{(p)}|^2$:

$$R(\alpha_0, \lambda) = \left(|r_{(s)}(\alpha_0, \lambda)|^2 + |r_{(p)}(\alpha_0, \lambda)|^2\right)/2 \quad (8)$$

The final value characterizing the quality of the reflective film is the integral reflection coefficient $R_I$:

$$R_I = \int_{\lambda_l}^{\lambda_u} \int_0^{\pi/2} \Omega(\alpha_0) \cdot I_{ir}(\lambda) \cdot R(\alpha_0, \lambda) d\lambda\, d\alpha_0, \quad (9)$$

where $I_{ir}(\lambda)$ is the spectral characteristic of the radiation source (Fig. 2), and $\Omega(\alpha_0)$ is the angular dependence of the radiation flow, or the radiation directional diagram, or the luminous intensity coefficient, which depends on the mutual location and geometric characteristics of the device and the radiation source.

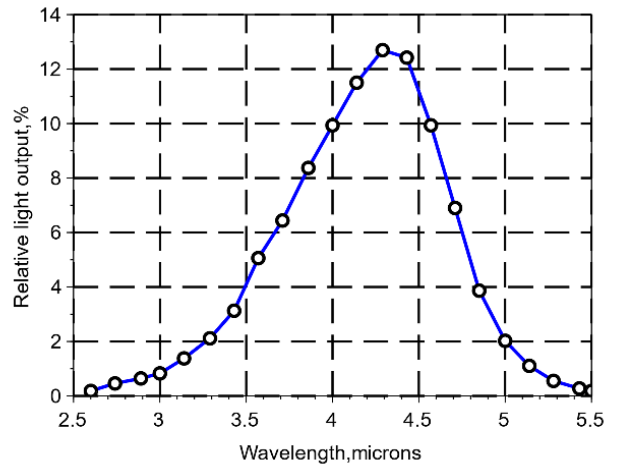


**Fig. 2.** Emission spectrum of the infrared LED from the L15895 series, manufactured by Hamamatsu.

### 1.3. Characteristics of the source of optical radiation

In every real case (except for the use of a completely black body model), it is very difficult to determine the coefficient of thermal radiation of a body. Therefore, the laws of radiation are used only in the case of the use of special models. Such methods can be applied for the approximate determination of the expected radiation parameters of real bodies.

To calculate the transmission spectra of films the spectral composition of the radiation falling on the film is taken into account. This characteristic is well known in solar energy, and by analogy we can write:

$$T_{ph} = \frac{\int_{\lambda_{min}}^{\lambda_{max}} T(\lambda) I_s(\lambda) d\lambda}{\int_{\lambda_{min}}^{\lambda_{max}} I_s(\lambda) d\lambda}, \quad (10)$$

where the interval of radiation, which is converted by the device into a photocurrent, is given by the lower and upper wavelengths: $\lambda \in [\lambda_{min}; \lambda_{max}]$, the spectral composition of the radiation source $I_s(\lambda)$ and the spectral characteristic of the transmission of the optical film $T(\lambda)$.

Another important characteristic of the radiation source is the angular dependence of the radiation intensity (the so-called optical field of view).

The technical characteristics of the infrared radiation source are obtained on the basis of the data of the infrared

LED manufacturer Hamamatsu [5]. The emission spectrum of the product from the L15895 series, which has an emission peak at a wavelength of 4.3 microns, and which is suitable for use in optical gas sensors, is shown in Fig. 2.

A significant difference between the application of the matrix method for photovoltaic solar energy devices and detectors of radiation generated by artificial sources is the need to take into account the unevenness of the directional pattern for artificial radiation sources. This is due to the fact that the surface of the Sun radiates according to a law close to the Lambertian law, the brightness of which does not depend on the direction of observation.

Modern production technologies provide an opportunity to form narrowly collimated beams of infrared radiation with an angular width of the cone of 10°;+10° in order. Such a device is described in [6], where the use of an infrared light-emitting diode in wireless optical communication is described. Another common model of the source of infrared radiation in instrumentation is the black body model given in [7] for the infrared optical sensor AK9710ADF01 produced by Asahi Kasei Microdevices, which is used to measure the concentration of carbon dioxide. The ray propagation scheme for this model is shown in Fig. 3. The proposed hybrid microsystem for biomedical applications can be used to estimate the intensity of radiation absorbed by the diode [12].

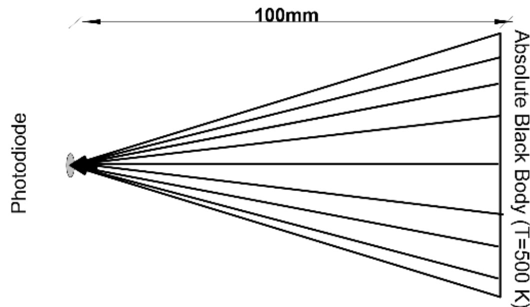


**Fig. 3.** Emission spectrum of the infrared LED from the L15895 series, manufactured by Hamamatsu.

Based on the distribution scheme, it becomes clear that the distribution of the intensity of incident radiation in the plane of the photodiode surface can be neglected (the area of the photosensitive surface for the photodiode AK9710ADF01 [7] is $1.21\ mm^2$).

An important feature of the model of an absolute black body is that the energy or spectral characteristics of radiation in any region of the optical range from 0.2 μm to 100 μm can be calculated based on the known temperature of its emitting surface and dimensions (diameter of the output aperture). If the surface of the photoreceptor is at a distance $L$ from the emitter, then the energy illuminance $E_e$ is calculated by the formula:

$$E_e = \frac{\sigma \cdot F \cdot (\varepsilon_1 T_1^4 - \varepsilon_0 T_0^4)}{\pi L^2}, \tag{11}$$

where $L = 100\ mm$ is the distance from the emitting surface to the surface of the photodiode, $F$ is the area of the radiating surface, which according to the scheme is:

$$F = \pi \cdot d^2/_4 \approx 3.87 \times 10^{-4}\ m^2; \tag{12}$$

where $T_1 = 500\ K$ is absolute blackbody temperature, $T_0 = 300\ K$ is the temperature of the surface of the photodiode (we assume that the device is not cooled), $\varepsilon_1 = 1$ is absolute black body emissivity, $\varepsilon_0$ is the emissivity of the photodiode surface, $\sigma = 5.67 \times 10^{-8}\ \text{Вт} \cdot \text{м}^{-2} \cdot \text{К}^{-4}$ is Stefan-Boltzmann constant.

Based on expression (11), we see that the emissivity $\varepsilon_0$ becomes a parameter of the problem, since, in accordance with Kirchhoff's law, it is related to the value of the film reflection coefficient $R$, which we optimize.

The maximum difference in the path of the rays from the surface of the absolutely black body to the surface of the photodiode is approximately equal $\sqrt{100^2 + 11.1^2} - 100 \approx 0.61\ \text{мм}$. With such a stroke difference, the difference in the intensity of the light flux absorbed by carbon dioxide is negligibly small, so we can ignore the angular dependence $\Omega(\alpha_0)$ in formula (9), and set the frequency range of integration according to the scheme in Fig. 3 equal to $\left[-arctg\left(\frac{11.1}{100}\right); arctg\left(\frac{11.1}{100}\right)\right] \approx$ $\approx [-6.3°; 6.3°]$.

## II. Results and discussion

The results of modelling reflection coefficients for light with parallel and perpendicular polarization are shown in Fig. 4.

The modelling of the film showed that both for light with parallel and perpendicular polarization, there is a significant dependence of the reflection coefficients on the wavelength even for a small range that corresponds to the spectral intensity of an infrared LED (Fig. 2), and for angles of incidence in the range$[-6.3°; 6.3°]$ reflection coefficients do not change. But at the same time, the reflection coefficient from the entire film has quite high values. Therefore, the thickness of the film layers should be optimized. For this, one optimization parameter is chosen, which is equal to the reference wavelength $l_0$, relative to which the thickness of each layer is calculated, and on which the total interference effect for the entire film depends (13):

$$d_i = \frac{l_0}{4n_i}, i = 1,2,3,4. \tag{13}$$

Criterion (13) is a well-known criterion for determining the optimal thickness of a single-layer film.

Further, the $d_i$ values are used in formula (3), which determines the optical thickness of each layer, which now depends on the optimization parameter - the reference wavelength $l_0$.

To find the optimal solution, the integral reflection coefficients for waves with parallel and perpendicular polarization, which depend on the optimization parameter $l_0$, are calculated. The reflection coefficients for values of the parameter $l_0$ are from the range [0.1 μm; 8 μm].

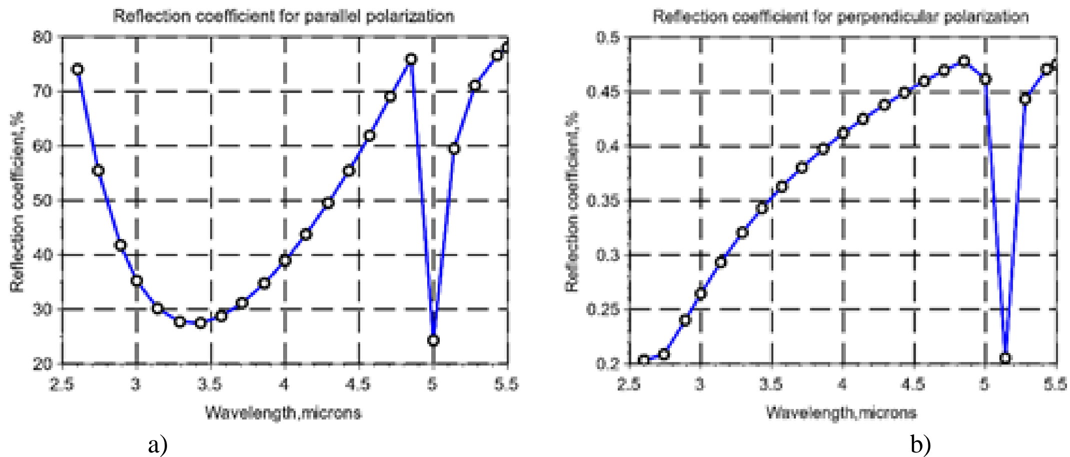


a) b)

**Fig. 4.** The absolute values of the squares of the reflection coefficients for light with parallel $|r_{(s)}|^2$ (a) and perpendicular $|r_{(p)}|^2$ (b) respectively.

The result of solving this optimization problem is shown in Fig. 5.

According to this result, the optimal wavelength for adjusting the layer thicknesses is $l_o \approx 820\ nm$. Then the thicknesses of the layers of silicon dioxide, silicon oxide, silicon suboxide, and germanium are: $l_{SiO_2} \approx 140\ nm$; $l_{SiO} \approx 105\ nm$; $l_{SiO_{0<x<1}} \approx 75\ nm$; $l_{Si} \approx 63\ nm$. The integral reflectance for parallel polarized light is 40%, with perpendicularly polarized light is 3%, and for unpolarized light the reflectance is 22%.

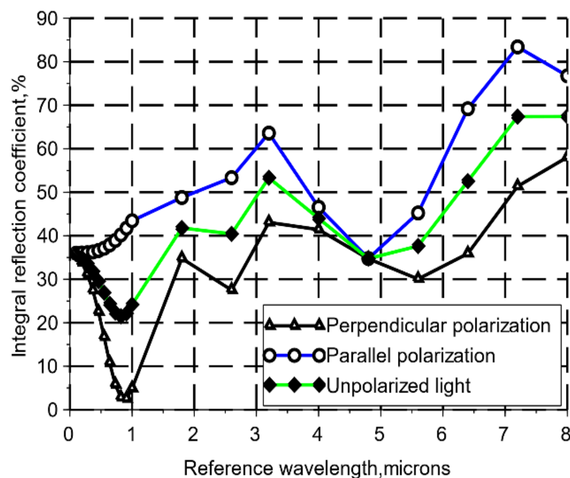


**Fig. 5.** Optimization of reflection coefficients for waves with perpendicular, parallel polarization and unpolarized light by reference wavelength.

The spectral composition of reflected radiation for parallel and perpendicular polarization, as well as for unpolarized light for a film with an optimized layer thickness, is shown in Fig. 6.

Based on the obtained results (Fig. 6), it can be concluded that the optimized films continue to show a significant difference for the reflection coefficients of waves with parallel and perpendicular polarization. This may be the key to further optimization when using a polarized light photodiode for operation, but this will reduce the overall emission intensity. The spectral composition of the radiation reflected from the film (Fig. 6) is almost identical to the spectrum of the incident radiation (Fig. 2).

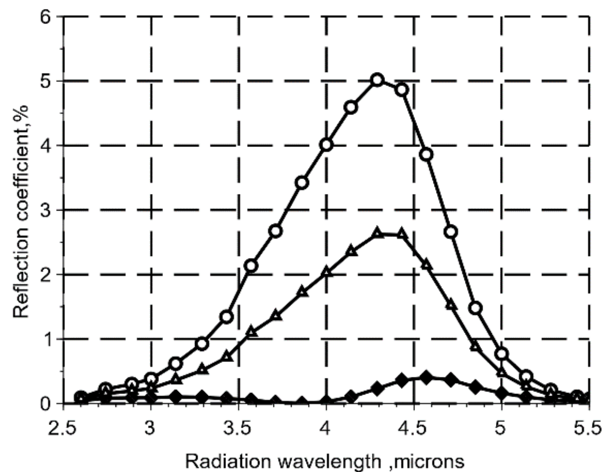


**Fig. 6.** Spectral composition of reflected radiation for parallel and perpendicular polarization, and unpolarized light for a film with optimized layer thickness.

The integral reflection coefficient for unpolarized radiation is 22%, which is comparable to the data given in the technical characteristics for infrared radiation sensors.

# Conclusions

Based on the study of interference processes of reflected and refracted radiation in the infrared wavelength ranges [2.5 µm; 5.5 µm] and angles of incidence [0°;6°], the reflection coefficients of waves with parallel and perpendicular polarization for a four-layer film ($SiO_2$, SiO, $SO_{1<x<2}$ and Si) on the surface of indium antimonide (InSb) are determined by the matrix method. The analysis of the results shows that for the studied range of incidence angles, the angular dependence of the reflection coefficient is practically not observed. Calculated integral reflection coefficients for the entire investigated range of wavelengths. The integral coefficient for waves with parallel polarization exceeds

the coefficient for waves with perpendicular polarization by 40%. At the same time, the integral coefficient for waves with perpendicular polarization does not exceed 0.5%. For a source of unpolarized light (with the same intensity of light with parallel and perpendicular polarization), calculations are made of the optimal thickness of four layers, which turned out to be 140 ($SiO_2$), 105 (SiO), 75 ($SO_{1<x<2}$) and 63 (Si) nm. At the same time, the integral reflection coefficient for unpolarized light is 22%, and the total thickness of the film is 383 nm, while the thickness of the antireflective film intended for detection in the visible and infrared ranges was 740 nm [9].

***Politanskyi Ruslan*** – Doctor of technical sciences, professor of the department of radio engineering and information security;
***Kogut Igor*** – Doctor of technical sciences, professor, head of the department of computer engineering and electronics;
***Vistak Maria*** – Doctor of technical sciences, professor of the department of biophysics;
***Mykytyuk Zinoviy*** – doctor of physical and mathematical sciences, professor of the department of electronic devices;
***Shymchyshyn Olha*** – candidate of technical sciences, associate professor of the department of electronic engineering;
***Diskovskyi Ivan*** – candidate of medical sciences, assistant of the department of dermatology and venereology.

[1] R.L. Politanskyi, M.V. Vistak, G.I. Barylo, A.S. Andrushchak. *Simulation of anti-reflecting dielectric films by the interference matrix method*,Opt Mater, 102, 109782 (2020); https://doi.org/10.1016/j.optmat.2020.109782.
[2] E. Zäll, M. Järn, S. Karlsson, H. Tryggeson, M. Tuominen, M. Sundin, T. Wågberg, *Aerosol-Based Deposition of Broadband Antireflective Silica Coating with Closed Mesoporous Structure*, Sol. Energy Mater. Sol. Cells, 250, 112078 (2023); https://doi.org/10.1016/j.solmat.2022.112078.
[3] Z.D. Shui, S. Wang, Z. Yang, D. Wang, B.Z. Tian, S. Luo, Z.Wang, L. Yang, *Polarization-sensitive self-powered tellurium microwire near-infrared photodetector,* Appl. Phys. Lett., 122, 101902 (2023); https://doi.org/10.1063/5.0142575.
[4] L. Wang, J. Zhang, S. Zhang, E. Song. *Self-powered photodetectors based on Er-doped $MoS_2$ for NIR photo-communication and laser calibration*, Appl. Phys. Lett., 122, 251104 (2023); https://doi.org/10.1063/5.0151055.
[5] L. Ottaviano, D. Mastrippolito, *The future ahead gas sensing with two-dimensional materials*, Appl. Phys. Lett., 123, 050502 (2023); https://doi.org//10.1063/5.0164342.
[6] X. Hu, K. Liu, Y. Cai, S.Q. Zang, T. Zhai. *2D Oxides for Electronics and Optoelectronics*, Small Sci., 2, 2200008 (2022); https://doi.org/10.1002/smsc.202200008.
[7] F. Xie, M. Ren, W. Wu, W. Cai, J. Xu. *Chiral metasurface refractive index sensor with a large figure of merit*, Appl. Phys. Lett., 122, 071701 (2023); https://doi.org/10.1063/5.0135657.
[8] Y.Y. Sun, C.A. Yang, Dn. Zeng, G. Wang, Q.X. Jia, C. Guo, Y. Lv., Z. Jiang, X. Han, D. Jiang, Z.C. Niu. *Broadband antireflection coating for the near-infrared InAs/GaSb Type-II superlattices photodetectors by lift-off process*, Proc. of SPIE., 10826, 108261Z-1 (2023); https://doi.org/10.1117/12.2509181. assignee. Wideban
[9] I. Kasai, H.L. Hettich, S.L. Lawrence, J.E. Randolph, S.L. Obispo, inventors; Santa Barbara *Research Center, d ant-reflection coating for indium antimonide photodetector device and method of forming the same*. US patent 934, 146 (1992, Aug 21).
[10] Web-source: https://www.hamamatsu.com/content/dam/hamamatsuphotonics/sites/documents/99_SALES_LIBRARY/ssd/l15893_series_etc_kled1085e.pdf.
[11] https://www.akm.com/eu/en/products/co2-sensor/lineup-co2-sensor/sensor-element/ak9710adf01/.
[12] B. S. Dzundza, I.T. Kohut, V.I. Holota, L.V. Turovska, M.V. Deichakivskyi, *Principles of construction of hybrid microsystems for biomedical applications*, Physics and Chemistry of Solid State, 23(4), 776 (2022); https://doi.org/10.15407/fm30.02.303.

Р. Л. Політанський[1], І.Т. Когут[2], М.В. Вісьтак[3], З.М. Микитюк[4], О. Шимчишин[4], І. Дісковський[3]

# Моделювання багатошарової високотехнологічної плівки для фотодетектора інфрачервоного діапазону (3.5-5.0 мкм)

[1]*Чернівецький національний університет імені Юрія Федьковича, Чернівці, Україна*
[2]*Прикарпатський національний університет імені Василя Стефаника, Івано-Франківськ, Україна, igor.kohut@pnu.edu.ua*
[3]*Львівський національний медичний університет імені Данила Галийького, , Україна*
[4]*Національний університет «Львівська політехніка», Львів, Україна*

У роботі проведене дослідження властивостей антивідбиваючої плівки для фотодетектора, виготовленого із антимоніду індію (InSb), налаштованого на пропускання у інфрачервоному діапазоні (3.5-5.0 мкм), що співпадає з піком поглинання вуглекислого газу ($CO_2$). Плівка являє собою чотиришарове покриття, утворене такими матеріалами: діоксид кремнію ($SiO_2$), монооксид кремнію (SiO), субоксид кремнію($SiO_{1<x<2}$) та кремній (Si), які розміщені у порядку збільшення показника заломлення: 1.45, 1.9, 2.6 і 3.2. Таким чином плівка забезпечує зростання показника заломлення від 1 до значення, наближеного до показника заломлення активного матеріалу фотодіода (4.0). За допомогою матричного методу проведене обчислення комплексного коефіцієнту відбивання світла для перпендикулярної та паралельної поляризації у діапазоні довжини хвилі та кутів падіння на поверхню плівки, що відповідають характеристикам сенсора інфрачервоного випромінювання. Діапазон кутів вибраний на основі геометричних характеристик інфрачервоного недисперсійного сенсора AK9710ADF01, розробленого компанією Asahi Kasei. Спектральний склад світла визначений за характеристиками інфрачервоного світодіода серії L15895, виготовленого компанією Hamamatsu. В результаті проведених досліджень підібрано оптимальні значення товщин шарів, які забезпечують коефіцієнт відбивання 22% для неполяризованого випромінювання, що порівняно із значеннями, які властиві сучасним фотоприймачам інфрачервоного діапазону. Разом із тим зроблено висновок про значно більші значення коефіцієнту відбиття для хвиль із паралельною поляризацією (на 40% на центральній довжині хвилі), ніж для хвиль із перпендикулярною поляризацією.

**Ключові слова:** хвильова інтерференція, матричний метод, інфрачервоний датчик, інфрачервоний світлодіод